Eur. Phys. J. A **17**, 159–165 (2003)
DOI 10.1140/epja/i2002-10156-y

THE EUROPEAN PHYSICAL JOURNAL A

Inelastic excitation of ^{187}Re

T. Shizuma[1,a], Y. Toh[1], M. Oshima[1], M. Sugawara[2], M. Matsuda[1], T. Hayakawa[1], M. Koizumi[1], A. Osa[1], Y.H. Zhang[3], and Z. Liu[3]

[1] Japan Atomic Energy Research Institute, Tokai, Ibaraki 319-1195, Japan
[2] Chiba Institute of Technology, Narashino, Chiba 275-8588, Japan
[3] Institute of Modern Physics, Chinese Academy of Sciences, Lanzhou 730000, China

Received: 12 December 2002 / Revised version: 18 February 2003 /
Published online: 13 May 2003 –
Communicated by D. Schwalm

Abstract. Excited states in ^{187}Re populated by inelastic scattering of a 500 MeV ^{82}Se beam have been studied by means of in-beam γ-ray spectroscopy. Levels built on the $5/2^+[402]$ and $9/2^-[514]$ one-quasiparticle states were measured up to $I^\pi = (21/2^+)$ and $(21/2^-)$, respectively. In addition, several new levels including an isomer at 1682 keV with a half-life of 114(23) ns have been found. Quasiparticle configurations of the levels and the transition rates are discussed.

PACS. 21.10.Tg Lifetimes – 23.20.Lv Gamma transitions and level energies – 27.70.+q $150 \leq A \leq 189$

1 Introduction

Nuclear-structure studies of states with medium to high spins in ^{187}Re have been limited because this nucleus resides at the line of β-stability, and few heavy-ion fusion-evaporation reactions would populate those states. To date only low-spin levels have, therefore, been known from studies on β decay of ^{187}W [**?**], ^{186}W(α, t), ^{186}W$(^3\mathrm{He}, \mathrm{d})$ [**?**], and ^{187}Re$(\mathrm{d}, \mathrm{d}')$ [**?**] reactions. In order to investigate higher-spin states, we employed an inelastic-scattering reaction with a heavy-ion beam. This type of reaction has been proven to be useful for the population of levels of medium to high spins in heavier stable isotopes [**?**].

The nucleus ^{187}Re lies in the region where many high-Ω orbitals are close to both the proton and neutron Fermi surfaces. High-$K(=\sum \Omega)$ multi-quasiparticle states formed by stretched coupling of these high-Ω quasiparticles, therefore, can compete with collectively excited states nearby a yrast line [**?**] (K is defined as a projected component of the total angular momentum on the nuclear symmetry axis). Transitions depopulating such states often involve large spin/K changes, low transition energies, parity change, or combination of these, making the initial state to be an isomer with a comparatively long half-life.

In this paper, we present results of the inelastic-scattering experiment on ^{187}Re, which include the identification of a new isomer based on three-quasiparticle excitation.

[a] e-mail: shizuma@popsvr.tokai.jaeri.go.jp

2 Experiments

A 500 MeV ^{82}Se beam derived from the tandem and booster accelerator at Japan Atomic Energy Research Institute was used to bombard a thick target (26 mg/cm^2) of natural Re. The beam energy was selected as about 15% higher than the Coulomb energy for the ^{82}Se + ^{187}Re system. Emitted γ-rays were detected by the GEMINI Ge detector array [**?**] consisting of twelve Compton-suppressed HP-Ge detectors, positioned at 32° (2 detectors), 58° (2), 90° (4), 122° (2) and 148° (2) with respect to the beam axis. Events were recorded on magnetic tapes when two or more Ge detectors were detected in coincidence. Relative Ge times between coincident γ-rays were also measured. The time window was set to 200 ns so that half-lives less than $\sim$ 100 ns could be extracted. A total of 1.5×10^8 coincidence events were collected. The energy calibration was made by using ^{133}Ba and ^{152}Eu standard sources. Two-dimensional E_γ-E_γ matrices of both the prompt-prompt and prompt-delayed coincidence were created to construct the level scheme.

The directional correlations of γ-rays de-exciting oriented states (DCO) ratio [**?**,**?**] defined below was used to deduce transition multipole orders:

$$R_{\mathrm{DCO}} = \frac{I_\gamma \text{ at } 32°(\text{or } 148°) \text{ gated on } \gamma_{\mathrm{G}} \text{ at } 90°}{I_\gamma \text{ at } 90° \text{ gated on } \gamma_{\mathrm{G}} \text{ at } 32°(\text{or } 148°)}.$$

Since the angle of 148° is equivalent to that of 32° [**?**], the corresponding events were summed in the DCO matrices to increase the statistics. In the DCO analysis, stretched

Table 1. Energies, level assignments, relative intensities, and DCO ratios for the γ-ray transitions in ^{187}Re.

E_γ(keV)	E_i(keV)	J_i^π	$\rightarrow$	J_f^π	I_γ	DCO
72	206.2	$9/2^-$	$\rightarrow$	$7/2^+$		
(91)	1474.2	$19/2^-$	$\rightarrow$	$19/2^-$		
134.2(1)	134.2	$7/2^+$	$\rightarrow$	$5/2^+$	655(21)	0.44(1)
155.2(2)	1474.2	$19/2^-$	$\rightarrow$	$(17/2^-)$	0.4(4)	
169.8(1)	303.9	$9/2^+$	$\rightarrow$	$7/2^+$	1000(30)	0.54(1)
182.3(1)	388.6	$11/2^-$	$\rightarrow$	$9/2^-$	7(1)	
188.9(1)	1870.4		$\rightarrow$	$(19/2^+)$	0.62(7)	
192.3(2)	1034.6	$(11/2^+)$	$\rightarrow$	$(9/2^+)$	2(1)	
204.9(1)	508.9	$11/2^+$	$\rightarrow$	$9/2^+$	337(10)	
206.2(1)	206.2	$9/2^-$	$\rightarrow$	$5/2^+$		
207.3(1)	1681.6	$(19/2^+)$	$\rightarrow$	$19/2^-$	1.3(1)	
214.8(1)	603.4	$13/2^-$	$\rightarrow$	$11/2^-$	8(1)	
223.5(2)	1257.7	$(13/2^+)$	$\rightarrow$	$(11/2^+)$	2.4(2)	
236.1(1)	839.5	$15/2^-$	$\rightarrow$	$13/2^-$	3.4(2)	0.84(12)
236.4(1)	745.3	$13/2^+$	$\rightarrow$	$11/2^+$	140(4)	
249.9(1)	1042.5	$(15/2^-)$	$\rightarrow$	$(13/2^-)$	2.1(2)	
253.8(2)	1511.5	$(15/2^+)$	$\rightarrow$	$(13/2^+)$	1.7(1)	
267.2(1)	1106.7	$17/2^-$	$\rightarrow$	$15/2^-$	2.4(1)	
270.2(1)	1015.5	$15/2^+$	$\rightarrow$	$13/2^+$	45(2)	0.96(3)
276.4(1)	1319.0	$(17/2^-)$	$\rightarrow$	$(15/2^-)$	1.5(1)	
276.8(1)	1383.5	$19/2^-$	$\rightarrow$	$17/2^-$	0.59(7)	
290.4(1)	1673.9	$(21/2^-)$	$\rightarrow$	$19/2^-$	0.49(5)	
294.9(1)	1310.5	$17/2^+$	$\rightarrow$	$15/2^+$	13(1)	0.95(2)
304.0(1)	303.9	$9/2^+$	$\rightarrow$	$5/2^+$	173(6)	0.80(3)
328.8(1)	1639.4	$19/2^+$	$\rightarrow$	$17/2^+$	1.8(1)	
329.1(1)	2199.5		$\rightarrow$		0.7(1)	
342.9(1)	1982.4	$(21/2^+)$	$\rightarrow$	$19/2^+$	0.3(1)	
367.6(1)	1474.2	$19/2^-$	$\rightarrow$	$17/2^-$	1.9(1)	0.9(1)[a]
374.7(1)	508.9	$11/2^+$	$\rightarrow$	$7/2^+$	130(4)	
397.5(2)	603.4	$13/2^-$	$\rightarrow$	$9/2^-$	0.7(3)	
404.0(1)	792.6	$(13/2^-)$	$\rightarrow$	$11/2^-$	28(1)	
439.1(1)	1042.5	$(15/2^-)$	$\rightarrow$	$13/2^-$	1.2(1)	
441.3(1)	745.3	$13/2^+$	$\rightarrow$	$9/2^+$	86(3)	
450.9(1)	839.5	$15/2^-$	$\rightarrow$	$11/2^-$	1.6(2)	
453.4(1)	842.1	$(9/2^+)$	$\rightarrow$	$11/2^-$	1.5(1)	
503.3(1)	1106.7	$17/2^-$	$\rightarrow$	$13/2^-$	1.2(1)	1.1(1)
506.7(1)	1015.5	$15/2^+$	$\rightarrow$	$11/2^+$	37(1)	
526.4(1)	1319.0	$(17/2^-)$	$\rightarrow$	$(13/2^-)$	0.6(1)	
544.0(1)	1383.5	$19/2^-$	$\rightarrow$	$15/2^-$	0.32(10)	
565.2(1)	1310.5	$17/2^+$	$\rightarrow$	$13/2^+$	13(1)	1.1(1)
(567)	1673.9	$(21/2^-)$	$\rightarrow$	$17/2^-$		
586.3(1)	792.6	$(13/2^-)$	$\rightarrow$	$9/2^-$	5(1)	
623.7(2)	1639.4	$19/2^+$	$\rightarrow$	$15/2^+$	1.2(2)	
634.8(1)	1474.2	$19/2^-$	$\rightarrow$	$15/2^-$	0.10(7)	
645.4(1)	1034.6	$(11/2^+)$	$\rightarrow$	$11/2^-$	2.0(2)	
707.8(3)	842.1	$(9/2^+)$	$\rightarrow$	$7/2^+$	9(1)	
731.2(2)	1034.6	$(11/2^+)$	$\rightarrow$	$9/2^+$	0.7(2)	
748.6(2)	1257.7	$(13/2^+)$	$\rightarrow$	$11/2^+$	0.7(2)	
842.1(3)	842.1	$(9/2^+)$	$\rightarrow$	$5/2^+$	5(1)	
868.5(2)	1257.7	$(13/2^+)$	$\rightarrow$	$11/2^-$	1.2(1)	
899.9(2)	1034.6	$(11/2^+)$	$\rightarrow$	$7/2^+$	1.7(1)	
907.4(2)	1511.5	$(15/2^+)$	$\rightarrow$	$13/2^-$	0.66(10)	
953.2(4)	1257.7	$(13/2^+)$	$\rightarrow$	$9/2^+$	0.7(3)	

[a] $\Delta I = 1$ transitions are used as gates.

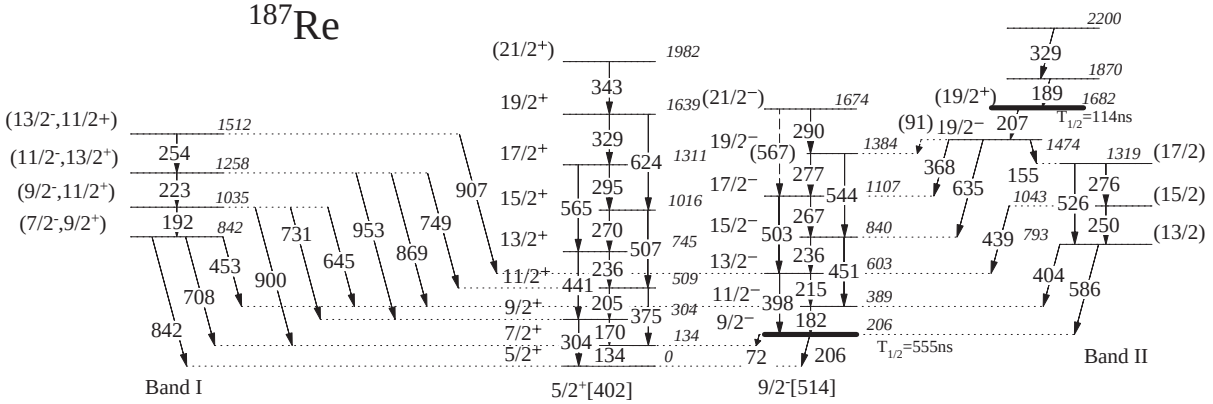

Fig. 1. A level scheme of ^{187}Re.

$\Delta I = 2$ transitions close to the γ-ray of interest are generally used as gates. In this case, the DCO ratios fall into unity for stretched quadrupole ($\Delta I = 2$), unstretched dipole ($\Delta I = 0$) transitions, and ~ 0.6 for stretched dipole ($\Delta I = 1$) transitions. For mixed $\Delta I = 1$ transitions, the DCO ratios depend on the the mixing ratio δ. However, when $E2$ transitions are weak, $\Delta I = 1$ transitions may be used as gates. In this case, the DCO ratios are around unity for $\Delta I = 1$ transitions, and ~ 1.7 for $\Delta I = 2$ transitions. In addition, the presence of both cascade ($\Delta I = 1$) and crossover ($\Delta I = 2$) transitions in the bands is used to confirm spin values. The information on γ-rays observed in ^{187}Re is summarized in table **??**.

3 Results

Figure **??** shows the proposed level scheme of ^{187}Re resulting from the present work. Two rotational bands based on one-quasiparticle excitation are labelled by their Nilsson configurations, while bands newly observed in this work are represented as Band I and Band II.

The rotational band tentatively assigned as the $5/2^+[402]$ one-quasiparticle configuration had been known up to $I^\pi = (13/2^+)$ [**?**]. Above this state, cascade ($\Delta I = 1$) and corresponding crossover ($\Delta I = 2$) transitions have been newly observed in coincidence with the known transitions in this band, as seen in fig. **??**(a). Consequently, we have extended this band up to $I^\pi = (21/2^+)$.

Several inter-band transitions from Band I have been observed to feed the $5/2^+[402]$ band. Spin and parity assignments of $7/2^+$, $7/2^-$ or $9/2^+$ are possible for the 842 keV level because it decays to the $I^\pi = 5/2^+$ and $7/2^+$ levels in the $5/2^+[402]$ band. The 842 keV level decays to a $I^\pi = 11/2^-$ state at 389 keV via a 453 keV transition. If the spin and parity of the 842 keV state were $7/2^+$, the 453 keV transition would have magnetic quadrupole character ($M2$). Since the $M2$ transition probabilities are normally very small, the $I^\pi = 7/2^+$ assignment would be rejected. We, therefore, take the spin and parity assignment of either $I^\pi = 7/2^-$ or $9/2^+$ for the 842 keV level.

Two levels at $E_x = 206$ and 389 keV were known as members of the $9/2^-[514]$ band [**?**], but no transition connecting these levels has been reported yet. The $I^\pi = 9/2^-$ bandhead has a half-life of 555 ns [**?**], and decays to the $I^\pi = 5/2^+$ and $7/2^+$ states in the $5/2^+[402]$ band with 206 and 72 keV transitions. Figure **??**(b) shows a spec-

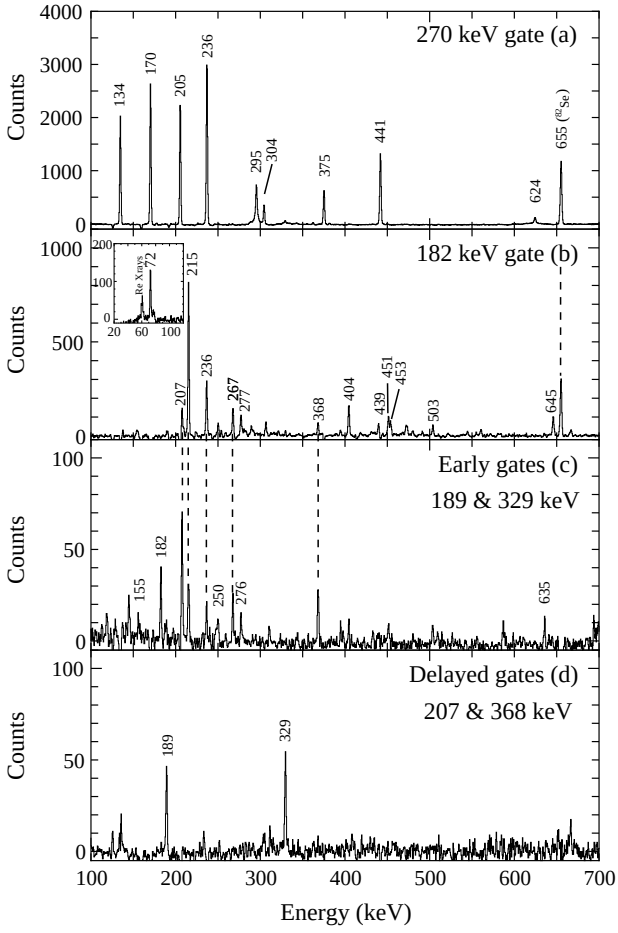

Fig. 2. Coincidence spectra gated on: (a) the 270 keV transition, showing the transitions in the $5/2^+[402]$ band, (b) the 182 keV transition, showing the transitions in the $9/2^-[514]$ band, (c) the early 189 and 329 keV transitions, showing the transitions below the isomer, and (d) the delayed 207 and 368 keV transitions, showing the transitions above the isomer.

Table 2. γ-ray intensity balances at the 1474 keV level.

Assumed multipolarity		Total intensity ratios[a]
155 keV	207 keV	
$E1$	$E1$	1.14(10)
$E1$	$M1$	1.80(14)
$E1$	$E2$	1.38(11)
$E1$	$M2$	4.75(42)
$M1$	$E1$	1.00(8)
$M1$	$M1$	1.59(12)
$M1$	$E2$	1.58(12)
$M1$	$M2$	4.18(35)
$E2$	$E1$	0.89(7)
$E2$	$M1$	1.40(10)
$E2$	$E2$	1.08(8)
$E2$	$M2$	3.90(32)
$M2$	$E1$	0.39(3)
$M2$	$M1$	0.47(4)
$M2$	$E2$	0.62(5)
$M2$	$M2$	1.62(10)

[a] Assuming $M1$ and $E2$ multipolarities for the 368 and 635 keV transitions.

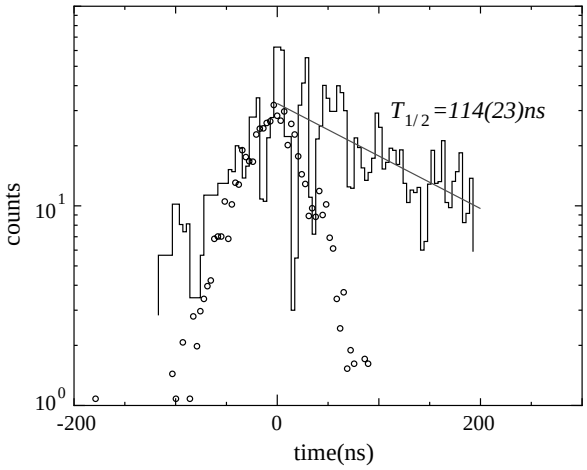

Fig. 3. A time difference spectrum between the 329 keV transition and the 215, 207, 329 keV transitions, showing the decay curve for the isomer. The time difference spectrum in prompt coincidence of the 270 and 236 keV transitions is also shown with open circles.

trum of γ-rays in coincidence with a 182 keV transition, which confirms that this γ-ray is a transition connecting the 206 and 389 keV levels. Inter-band transitions from Band I to these levels also support the present level placement. On top of the 389 keV state, rotational levels have been identified up to $I^\pi = (21/2^-)$.

A new level at 1474 keV has been found to decay to the $I^\pi = 15/2^-$ and $17/2^-$ states in the $9/2^-[514]$ band via 635 and 368 keV transitions. An unobserved 91 keV weak branch to the $I^\pi = 19/2^-$ state is implied from the coincidence data. In addition, a decay branch to Band II through a 155 keV transition has been found. From the decay branches to the $9/2^-[514]$ band members, the 1474 keV level is deduced to have spin and parity of either $17/2^+$, $17/2^-$ or $19/2^-$. The preferential population of the 1474 keV state with respect to the $9/2^-[514]$ band members would support the $19/2^-$ assignment. If the state had $I^\pi = 17/2^-$, an $E2$ transition to the $I^\pi = 13/2^-$ state in the $9/2^-[514]$ band would be observed. However, no such decay is found in the present data. Furthermore if the state were $I = 17/2$, both the 368 and 635 keV transitions would have dipole character, and it is difficult to explain their relative intensities. Experimentally, the 368 keV transition is observed about 20 times intense as the 635 keV transition. If both transitions were dipoles, the 635 keV transition would be about 5 times as intense as the 368 keV transition due to the E_γ^3-dependence on transition rates for dipole decays. This indicates that the 635 keV γ-ray has a quadrupole character. Consequently, the $I^\pi = 19/2^-$ assignment for the 1474 keV state is preferred.

From the analysis of a delayed coincidence spectrum of fig. **??**(c), a new isomer has been identified at 1682 keV, feeding the 1474 keV level by a 207 keV γ decay. For spin and parity assignments of this level, γ-ray intensity balances at the 1474 keV level have been examined assuming various multipolarities for the 155 and 207 keV transitions. Table **??** shows total intensity ratios of the 207 keV transition to the sum of the transitions depopulating the 1474 keV level. The ratio should be unity when correct multipolarities are used. Therefore $(M1, E1)$, $(E1, E1)$ or $(E2, E2)$ assignments are possible for the $(155, 207)$ keV transitions. However, the $(E2, E2)$ assignments can be rejected by the following reason. With this assignment, the bandhead spin and parity for Band II are $K^\pi = 11/2^-$, and then its decay to the $9/2^-[514]$ band via the 404 and 586 keV γ-rays would proceed by dipole transitions. The observed intensity ratio of $I_\gamma(586)/I_\gamma(404) = 0.18$ is however inconsistent with the value of 3.1 which is expected by the γ-ray intensity dependence for dipole transitions ($I_\gamma \propto E_\gamma^3$). Taking either $(M1, E1)$ or $(E1, E1)$ multipolarities for the $(155, 207)$ keV transitions, we made assignments of $I^\pi = (19/2^+)$ or $(21/2^+)$ for the 1682 keV isomer, and of $I = (17/2)$ for the 1319 keV level leading to the $K = (13/2)$ assignment for Band II. Here, the $I = 19/2$ assignment for the 1319 keV level can be rejected, since in this case the 586 keV transition requires a spin transfer of at least $3\hbar$. Above the 1682 keV isomer, two γ-rays at 189 and 329 keV are observed as shown in fig. **??**(d). The ordering of the levels is based on the transition intensities. No other information is obtained.

For the determination of a half-life of the 1682 keV isomer, a γ-ray time difference spectrum (fig. **??**) between the transitions above and below the isomer has been analyzed. By fitting the decay slope, a half-life of 114 ± 23 ns has been obtained.

Table 3. g_K values deduced from the branching ratios for the $5/2^+[402]$ and $9/2^-[514]$ bands in ^{187}Re.

Band	I_i	$E_\gamma(E2)$ (keV)	$E_\gamma(M1/E2)$ (keV)	λ	$\lvert g_K^{\rm exp} - g_R\rvert^{\rm (a)}$
$5/2^+[402]$	9/2	304	170	0.17(1)	1.2(1)
	11/2	375	205	0.39(2)	1.3(1)
	13/2	441	236	0.61(3)	1.3(1)
	15/2	507	270	0.82(4)	1.4(1)
	17/2	565	295	1.0(1)	1.5(1)
$9/2^-[514]$	13/2	398	215	0.08(4)	1.1(2)
	15/2	451	236	0.47(7)	0.70(5)
	17/2	503	267	0.50(5)	0.84(4)
	19/2	544	277	0.50(19)	1.0(2)

(a) $Q_0 = 5.8\ e$b [**?**] is used.

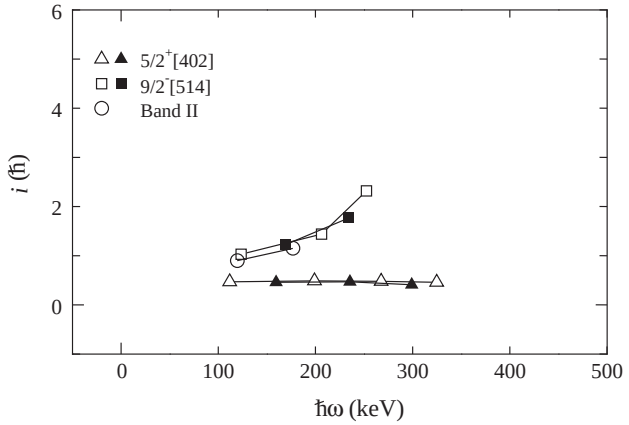

Fig. 4. Alignment plots for the bands observed in ^{187}Re. Harris parameters of $\mathfrak{J}_0 = 22.7\ \mathrm{MeV}^{-1}\cdot\hbar^2$ and $\mathfrak{J}_1 = 53.6\ \mathrm{MeV}^{-3}\cdot\hbar^4$ are used.

4 Discussion

4.1 Properties of the one-quasiparticle bands

In the cranked shell model [**?**] rotational alignments can be obtained by subtracting the aligned angular momentum of the reference configuration from the total aligned angular momentum $I_x[= \sqrt{I(I+1)-K^2}]$. In fig. **??**, rotational alignments for the bands observed in ^{187}Re are shown as a function of the rotational frequencies $\hbar\omega$ given in units of keV. Harris parameters used are $\mathfrak{J}_0 = 22.7\ \mathrm{MeV}^{-1}\cdot\hbar^2$ and $\mathfrak{J}_1 = 53.6\ \mathrm{MeV}^{-3}\cdot\hbar^4$ taken from averages of those for the ground-state bands in ^{186}W and ^{188}Os. In the calculation, we assume the K values fixed to the bandhead spins.

Both the one-quasiparticle bands show small initial alignments, which are consistent with the proposed configuration assignments of $5/2^+[402]$ and $9/2^-[514]$. The gradual increase in the alignments of the $9/2^-[514]$ band would be due to effects of the alignments to $i_{13/2}$ neutrons. Alignments for Band I and Band II are comparable to those for the $5/2^+[402]$ and $9/2^-[514]$ bands, indicating that these bands include no aligned quasiparticles such as $i_{13/2}$ neutrons and/or $h_{9/2}$ protons in the configuration, which will be discussed in sect. **??**.

Intensity ratios of $E2$ crossover to $M1(+E2)$ cascade transitions within a band can be used in the asymptotic limit to deduce g_K-factors. In the rotational model [**?**], the mixing ratio δ and the g_K-factor are deduced using the Clebsch-Gordon coefficients as

$$\frac{\delta^2}{1+\delta^2} = \lambda\,\frac{E_\gamma^5(I\to I-1)}{E_\gamma^5(I\to I-2)}\,\frac{\langle I\ K\ 2\ 0\mid I-1\ K\rangle^2}{\langle I\ K\ 2\ 0\mid I-2\ K\rangle^2}\ ,$$

and

$$\frac{(g_K-g_R)^2}{Q_0^2} = 0.289\,\frac{E_\gamma^2(I\to I-1)}{\delta^2 K^2}\,\frac{\langle I\ K\ 2\ 0\mid I-1\ K\rangle^2}{\langle I\ K\ 1\ 0\mid I-1\ K\rangle^2}$$

with the transition energies in MeV, where λ is the intensity ratio $T_\gamma(I\to I-2)/T_\gamma(I\to I-1)$, g_R the gyromagnetic ratio for the collective rotation, and Q_0 the intrinsic quadrupole moment. The values listed in table **??** have been extracted with the assumption that K is equal to the bandhead spin, and the quadrupole moment of $Q_0 = 5.8\ e$b taken from ref. [**?**].

The expected values of $(g_K - g_R) = 1.27\pm0.05$ for the $5/2^+[402]$ state and 1.00 ± 0.05 for the $9/2^-[514]$ state are well comparable with the experimental values (the uncertainties of ±0.05 are propagated from the assumption of $g_R = 0.30\pm0.05$ used in the $A\approx180$ region [**?**].) The present result therefore supports the previous configuration assignments for the one-quasiparticle bands.

4.2 Configuration assignments

In this section, quasiparticle configurations for the 1474 and 1682 keV states are given by comparison with the observed and calculated excitation energies. We have extracted excitation energies ($E_x^{\rm cal}$) by summing the energies of the constituent single-quasiparticle states and the associated energies to break the quasiparticle pairs. For neutrons, the experimentally known excitation energies for one-quasiparticle states in ^{187}Re were used, while averages of the observed excitation energies for the one-quasiparticle states in ^{185,187}W and ^{187,189}Os were used for protons. The neutron and proton pairing gap energies ($\Delta_{\rm n} = 866$ and $\Delta_{\rm p} = 744$ keV) were obtained from averages of those for ^{186}W and ^{188}Os using the 3rd-order odd-even mass differences [**?**], and were reduced by 20% for each quasiparticle broken pair to account for

the weaker pair field in the multi-quasiparticle configurations. Since the residual interaction known as the empirical Gallagher-Moszkowski (GM) rules [**?**] is an important factor to reproduce the observed excitation energies of multi-quasiparticle state, we estimated it by using the previous work by Jain *et al.* [**?**], and added the associated GM splitting energies $E^{\rm GM}$ to the calculated excitation energies.

The bandhead spins and parities for Band I and Band II have been assigned as $I^\pi = (7/2^-\text{or } 9/2^+)$ and $I = (13/2)$, respectively. The excitation energies of 842 and 793 keV are too low to be confirmed as three-quasiparticle excitation, and would suggest that these bands likely have vibrational character. For the detailed configuration, further experimental information is required to remove the ambiguity in the spin and parity assignments.

The 1474 keV level is confirmed as $K^\pi = 19/2^-$. No rotational band member built on this level is observed. However, its quasiparticle configuration may be deduced by comparison with the excitation energy. The lowest $K^\pi = 19/2^-$ state in ^{187}Re can be obtained by the following configuration:

$$\pi\{5/2^+[402]\} \otimes \nu 7^-\{3/2^-[512]\ 11/2^+[615]\}\,,$$

$$E_x^{\rm cal} + E^{\rm GM} = 1665 - 155 = 1510 \text{ keV}.$$

The two-quasineutron configuration of $\nu 7^-$ associated with the favoured spin-spin coupling is known at low excitation energies in ^{184}W (E_x = 1502 keV) [**?**], ^{186}Os (E_x = 1775 keV) [**?**] and ^{188}Os (E_x = 1771 keV) [**?**]. Therefore, the three-quasiparticle configuration obtained by coupling of $\nu 7^-$ to the ground-state configuration of $5/2^+[402]$ would be a low-lying state in ^{187}Re as well. We further note that $K^\pi = 6^-$ or $17/2^-$ states which have a similar configuration, *i.e.* $\nu 6^-\{3/2^-[512]\ 9/2^+[624]\}$ or $\pi 5/2^+[402] \otimes \nu 6^-$ are known at low excitation energies in ^{182}W (E_x = 1829 keV) [**?**], ^{184}Os (E_x = 1839 keV) [**?**], and ^{183}Re (E_x = 1763 keV) [**?**].

The 1682 keV isomeric level has been assigned as $K^\pi = (19/2^+)$ or $(21/2^+)$. The following configurations give the lowest $K^\pi = 19/2^+$ and $21/2^+$ states:

$$K^\pi{=}19/2^+, \pi\{9/2^-[514]\}\otimes\nu 5^-\{-1/2^-[510]11/2^+[615]\}\,,$$

$$E_x^{\rm cal} + E^{\rm GM} = 1920 - 150 = 1770 \text{ keV},$$

$$K^\pi{=}21/2^+, \pi\{9/2^-[514]\} \otimes \nu 6^-\{1/2^-[510]11/2^+[615]\}\,,$$

$$E_x^{\rm cal} + E^{\rm GM} = 1920 - 0 = 1920 \text{ keV}.$$

Both the configurations include the same single quasiparticles, but have the opposite spin-spin couplings for the neutron configuration associated with the favoured ($\nu 5^-$) and unfavoured ($\nu 6^-$) GM interaction. The favoured $\nu 5^-$ states are known in neighbouring nuclei of ^{184}W (E_x = 1285 keV) [**?**] and ^{186}Os (E_x = 1629 keV) [**?**]. Furthermore in ^{182}W [**?**], a pair of the favoured $\nu 4^-$ and unfavoured $\nu 5^-$ configurations of $\{1/2^-[510]\ 9/2^+[624]\}$ are observed at 1553 and 1809 keV, respectively, and would give the difference energy of 256 keV which could be associated with the GM residual interaction. Taking this advantage, we favour the $K^\pi = 19/2^+$ assignment for the 1682 keV isomeric state.

4.3 K-allowed and K-forbidden transitions

Electromagnetic transitions involving K changes equal to or less than the transition multipolarity, *i.e.*, $\Delta K \leq \lambda$, are allowed in the K-selection rule, otherwise the transitions ($\Delta K > \lambda$) are forbidden. Both types of transitions can be discussed in terms of hindrance factors $F = T^\gamma_{1/2}/T_{\rm W}$ or hindrance factors per degree of K-forbiddenness $f_\nu = F^{1/\nu}$, where ν is the order of K-forbiddenness, $T^\gamma_{1/2}$ and $T_{\rm W}$ are the partial γ-ray half-life and the corresponding Weisskopf single-particle estimate.

The 1474 keV level decays by the K-forbidden 155, 386 and 635 keV transitions with a short half-life of < 3 ns which is given by the upper limit for the present detection system. The 155 keV, $M1$ transition to the $K^\pi = (13/2^-)$ band has $f_\nu < 61$, while both the 368 keV, $M1$ and the 635 keV, $E2$ transitions to the $9/2^-[514]$ band have f_ν's < 10. These limits are along the systematic behavior, but are too high to make detailed discussion on the K quantum number in this nucleus.

The $K^\pi = (19/2^+)$ isomer at 1682 keV has been identified with $T_{1/2}$ = 114(23) ns. It decays to the $K^\pi = 19/2^-$ level at 1474 keV via the K-allowed $E1$ transition. The hindrance factor for this transition is obtained as $F = 5 \times 10^6$. This value is consistent with $F = 1.1{\times}10^6$ for a 115 keV, $E1$ decay of the 123 ns isomer in ^{185}Re [**?**], as well as the systematic value of $F \approx 10^3 \sim 10^7$ expected for K-allowed $E1$ transitions [**?**].

5 Conclusion

We have extended the $5/2^+[402]$ and $9/2^-[514]$ bands up to $I^\pi = (21/2^+)$ and $21/2^-$, respectively. The previous configuration assignments for these bands were confirmed by comparison with the observed and expected values of the rotational alignments and g_K-factors. Several new levels, including a $K^\pi = (19/2^+)$, 114 ns isomer, have been found, and their quasiparticle configurations were assigned on the basis of the simple multi-quasiparticle calculations. In addition, the hindrances measured for the K-allowed and K-forbidden transitions appeared to be consistent with the systematic values in the region.

We would like to thank the staff of JAERI tandem accelerator for providing the ion beam.

References

1. S. Yamada, S.P. Sud, Y. Miyatake, T. Hayashi, Nucl. Phys. A **332**, 317 (1979).
2. M.T. Lu, W.P. Alford, Phys. Rev. C **3**, 1243 (1971).
3. K.M. Bisgard, E. Veje, Nucl. Phys. A **103**, 545 (1967).

4. C. Wheldon, R. D'Alarcao, P. Chowdhury, P.M. Walker, E. Seabury, I. Ahmad, M.P. Carpenter, D.M. Cullen, G. Hackman, R.V.F. Janssens, T.L. Khoo, D. Nisius, C.J. Pearson, P. Reiter, Phys. Lett. B **425**, 239 (1998).
5. P.M. Walker, G.D. Dracoulis, Nature **399**, 35 (1999).
6. K. Furuno, M. Oshima, T. Komatsubara, K. Furutaka, T. Hayakawa, M. Kidera, Y. Hatsukawa, M. Matsuda, S. Mitarai, T. Shizuma, T. Saitoh, N. Hashimoto, H. Kusakari, M. Sugawara, T. Morikawa, Nucl. Instr. Methods A **421**, 211 (1999).
7. K.S. Krane, R.M. Steffen, R.M. Wheeler, Nucl. Data Tables **11**, 351 (1973).
8. L.P. Ekström, A. Nordlund, Nucl. Instrum. Methods A **313**, 421 (1992).
9. S. De Benedetti, F.K. McGowan, Phys. Rev. **71**, 185 (1947).
10. R.B. Firestone, *Table of Isotopes*, eighth edition (Wiley-Interscience, New York, 1996).
11. R. Bengtsson, S. Frauendorf, Nucl. Phys. A **327**, 139 (1979).
12. A. Bohr, B.R. Mottelson, *Nuclear Structure*, Vol. **2** (Benjamin, Reading, MA, 1975).
13. P.M. Walker, G.D. Dracoulis, A.P. Byrne, B. Fabricius, T. Kibèdi, A.E. Stuchbery, N. Rowley, Nucl. Phys. A **568**, 397 (1994).
14. G. Audi, A.H. Wapstra, Nucl. Phys. A **595**, 409 (1995).
15. C.J. Gallagher, S.A. Moszkowski, Phys. Rev. **111**, 1282 (1958).
16. K. Jain, O. Burglin, G.D. Dracoulis, B. Fabricius, N. Rowley, P.M. Walker, Nucl. Phys. A **591**, 61 (1995).
17. C. Wheldon, P.M. Walker, P.H. Regan, T. Saitoh, N. Hashimoto, G. Sletten, F.R. Xu, Nucl. Phys. A **652**, 103 (1999).
18. T. Shizuma, S. Mitarai, G. Sletten, R.A. Bark, N.L. Gjørup, H.J. Jensen, J. Wrzensinski, M. Piiparinen, Nucl. Phys. A **593**, 247 (1995).
19. C. Wheldon, G.D. Dracoulis, R.T. Newman, P.M. Walker, C.J. Pearson, A.P. Byrne, A.M. Baxter, S. Bayer, T. Kibèdi, T.R. McGoram, S.M. Mullins, F.R. Xu, Nucl. Phys. A **699**, 415 (2002).
20. C.S. Purry, P.M. Walker, G.D. Dracoulis, S. Bayer, A.P. Byrne, T. Kibèdi, F.G. Kondev, C.J. Pearson, J.A. Sheikh, F.R. Xu, Nucl. Phys. A **672**, 54 (2000).
21. T. Shizuma, G. Sletten, R.A. Bark, N.L. Gjørup, H.J. Jensen, S. Mitarai, M. Piiparinen, J. Wrzesinski Z. Phys. A **359**, 229 (1997).
22. K.E.G. Löbner, *The Electromagnetic Interaction in Nuclear Spectroscopy*, edited by W.D. Hamilton (North-Holland, Amsterdam, 1975) p. 141.